



**GEOLOGICAL SURVEY OF CANADA
OPEN FILE 7257**

**Geochemical anomalies in soils and uppermost siliciclastic
units overlying the Phoenix uranium deposit,
Athabasca Basin, Saskatchewan**

M.J. Power, K. Hattori, C. Sorba and E.G. Potter

2012



Natural Resources
Canada

Ressources naturelles
Canada

Canada



**GEOLOGICAL SURVEY OF CANADA
OPEN FILE 7257**

Geochemical anomalies in soils and uppermost siliciclastic units overlying the Phoenix uranium deposit, Athabasca Basin, Saskatchewan

M.J. Power¹, K. Hattori¹, C. Sorba² and E.G. Potter³

- 1- Dept. Earth Sciences, University of Ottawa, Ottawa, ON, K1N 6N5
- 2- Denison Mines Corp., 200-230 22nd St East, Saskatoon, SK, S7K 0E9
- 3- Geological Survey of Canada, 601 Booth St., Ottawa, ON, K1A 0E8

2012

©Her Majesty the Queen in Right of Canada 2012

This publication is available for free download through GEOSCAN (<http://geoscan.ess.nrcan.gc.ca/>)

doi:10.4095/291981

Recommended citation:

Power, M.J., Hattori, K., Sorba, C., and Potter, E.G., 2012. Geochemical anomalies in the soil and uppermost siliciclastic units overlying the Phoenix uranium deposit, Athabasca Basin, Saskatchewan; Geological Survey of Canada, Open File 7257, 36 p. doi:10.4095/291981

Publications in this series have not been edited; they are released as submitted by the author.

Table of Contents

Abstract	4
Introduction.....	5
Study Area and Uranium Mineralization	6
Topography	8
Climate.....	10
Soil Conditions.....	10
Sampling Methods	11
Analytical Methods.....	12
Leaches and Digestion	12
Mapping Software.....	13
Results.....	13
Discussion.....	29
Correlations between soil horizons and uppermost siliciclastic units	29
Implications for uranium exploration	29
Acknowledgments.....	29
References.....	30

Abstract

Many mineral deposits are concealed by younger rocks and unconsolidated glacial deposits, which make buried deposits difficult to explore using traditional exploration tools. Under the TGI4 program, this project is examining whether surficial geochemical anomalies exist for deeply buried uranium deposits. This study selected the Phoenix deposit on Denison Mines' Wheeler River Property, located in the southeastern Athabasca Basin, northern Saskatchewan. Discovered in 2008, the deposit currently has a National Instrument 43-101 indicated resource of approximately 40 million lbs U_3O_8 . The uranium oxide minerals are localized within four pods termed the A, B, C and D ore zones. These pods are located mostly along the unconformity between the crystalline basement rocks and overlying Athabasca sandstone units, approximately 400 metres below the surface. The region is characterized by gently rolling hills comprising glacial till and moraines ranging in thickness from 30 to 50 m, with continuous permafrost. A total of 226 soil samples (humus, E-, B-, and C-horizon) were collected from 59 sites along 3 transects at approximately 10 metre intervals over the "A" and "B" ore zones. The extensive transects facilitated sampling of both "mineralized" and "background values" in the study area.

Preliminary geochemical analyses of the samples revealed the presence of U, Mo, Co, Ag and W anomalies in humus, B-horizon soil and uppermost sandstone units overlying the ore zones and directly above the basement location of a nearby northeast-trending "WS Hanging Wall" shear zone. Concentrations in the surface media are up to 6 times background values for U, 5 times for Mo, 4 times for Co, 20 times for Ag and 18 times for W. The geochemical anomalies in the surface media and the uppermost sandstone units over the shear zone suggest that the fault has acted as a conduit for upward migration of fluids from the deposit. This preliminary study indicates that geochemical analysis of surface media is potentially an efficient and inexpensive exploration tool for detecting deep-seated uranium deposits.

Introduction

The Athabasca Basin in northern Saskatchewan, Canada is home to the world's largest and highest-grade unconformity-related uranium deposits, including the Phoenix Deposit at Wheeler River (Fig. 1). Exploration for new buried uranium deposits remains very difficult in the basin because of the lack of outcrop and the depth at which new deposits are being discovered (e.g. Shea Creek, Millennium and Centennial deposits ca. 650m, 700m and 800m, respectively; Jiricka, 2008). To support development of new exploration tools, this project commenced in September, 2011, under support from the Geological Survey of Canada through the Targeted Geoscience Initiative 4 (TGI-4) Program. The mandate of TGI4 is to develop new geoscience knowledge and techniques to increase exploration effectiveness in discovering deep minerals deposits. As such, a surficial geochemical survey over a known deposit was selected to develop geochemical methods for future exploration.

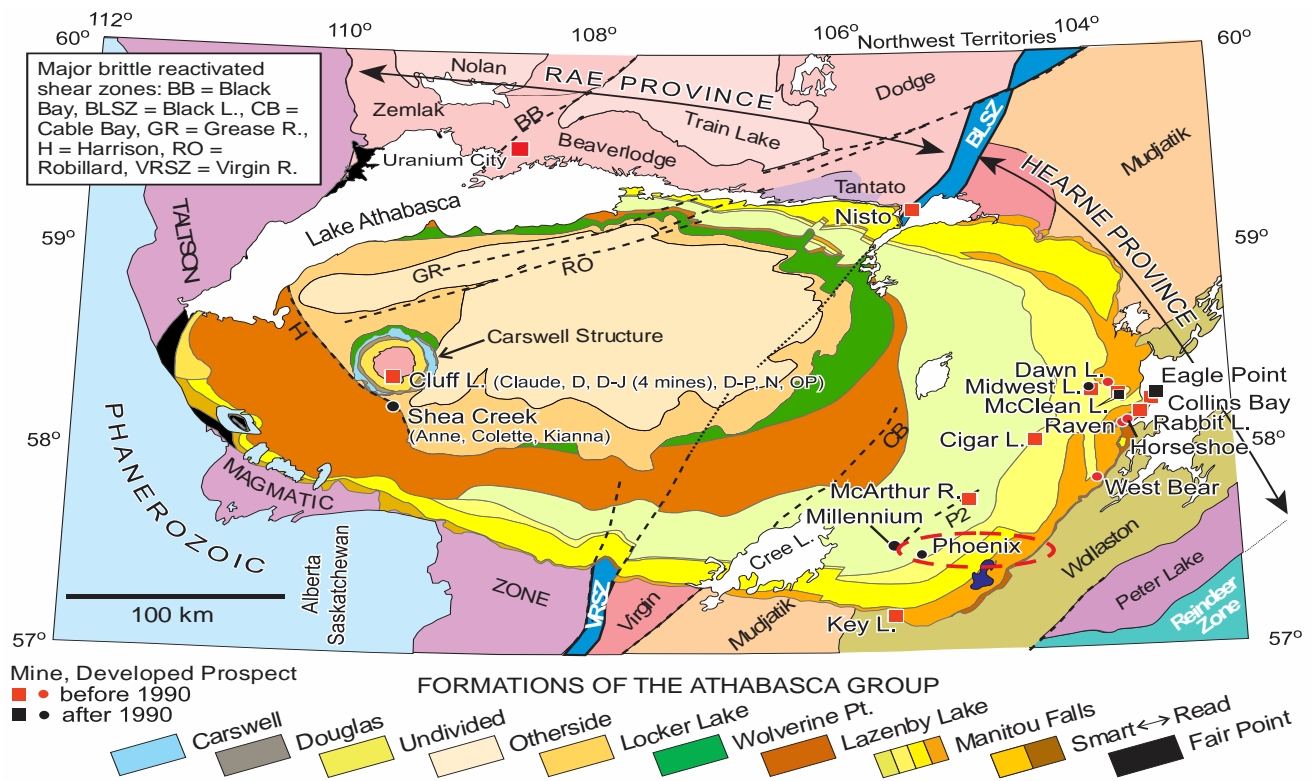


Figure 1: Location of the study area (dashed red oval) and Denison Mines Phoenix deposit in the eastern Athabasca Basin. Geology from Jefferson et al. (2007b).

The Proterozoic Athabasca Basin is a virtually undeformed, 1750 m thick, mainly fluvial sedimentary succession deposited between 1740 and 1500 Ma (Creaser and Stasiuk, 2007; Rainbird et al., 2007; Ramaekers et al., 2007). The dominantly siliciclastic Athabasca Group is subdivided into ten formations, which constitute four unconformity-bound sequences (Ramaekers et al., 2007; Yeo et al., 2007). These unconformably overlie metamorphic crystalline basement rocks consisting of Archean to Paleoproterozoic granitoid and supracrustal gneiss (Jefferson et al., 2007).

Basement rocks at Wheeler River property are part of the Paleoproterozoic Wollaston Domain of the Trans Hudson-Orogeny and consist of southeastwardly dipping metasedimentary rocks intercalated with granitoid gneiss (Yeo and Delaney, 2007). The metasedimentary rocks belong to the Paleoproterozoic Wollaston Supergroup and include graphitic and non-graphitic pelite, semipelitic

gneiss, felsic and quartz feldspathic gneiss, quartzite and rare calcisilicate gneiss. Near the Phoenix deposit, the Wollaston quartzite unit forms a prominent basement ridge that is entirely covered by the Athabasca Group and whose crest to the west of the study area is up to 200 metres above the adjacent basement surface. Garnetiferous pelite, graphitic pelite and pelite of the Wollaston Supergroup structurally overlie and are interpreted to be stratigraphically above the quartzite unit (Kerr, 2011).

At Wheeler River, only the Read and Manitou Falls formations of the Athabasca Group are preserved. As noted by Kerr (2011), the Read Formation (RD) can generally be subdivided into a lower unit of pebble-cobble conglomerate to pebbly sandstone and an upper unit of well sorted sandstone to pebbly sandstone. The Read Formation thins and disappears over the prominent quartzite ridge, suggesting the ridge represents a paleotopographic high. A breccia of centimetre- to metre-sized, angular quartzite blocks has been intersected in numerous drill holes along the western margin (footwall) of the quartzite ridge and is interpreted to represent a fault-scarp talus breccia (Bosman and Korness, 2007; Kerr, 2011). The Manitou Falls Formation comprises three members, the Bird (MFb), Collins (MFc) and Dunlop (MFd), which are differentiated by their proportions of conglomerate, and clay intraclasts (Ramaekers et al., 2007; Bosman and Korness, 2007). The conglomerate beds are distinguished not only by visual stratigraphic core logging but also by analysis of gamma-ray logs (Mwenifumbo et al., 2001). Both the RD and MFb contain upward fining conglomerate beds expressed as sharply elevated gamma-ray responses. The RD differs by having desiccation-cracked red mudstone interbeds, red mudstone intraclasts and less common heavy mineral laminae that generate less pronounced gamma-ray peaks, whereas the MFb has neither red beds nor intraclasts but very pronounced gamma-ray peaks associated with heavy mineral-rich conglomerate beds. The MFc gradationally overlies MFb and is characterized by quartz arenite with less than 2% conglomerate interbeds 2 cm or more thick, and less than 0.6 % clay intraclasts. The gradationally overlying MFd contains no conglomerate interbeds, and has greater than 0.6 % clay intraclasts (Ramaekers et al., 2007; Yeo et al., 2001; Bosman and Korness, 2007).

Study Area and Uranium Mineralization

The Wheeler River property has experienced approximately 30 years of uranium exploration, which culminated in the discovery of the Phoenix deposit in 2008 and was followed by one of the highest grade intersections in the basin the following summer (6.0 m of 62.6% U_3O_8 in Zone A, drill hole WR-273) (Fig. 2, Denison Mines Corp. Press Release 2008). The mineral resources drilled to date at the deposit are estimated to contain 35.6 (indicated) to 39.5 (inferred) million lbs of U_3O_8 in Zones A and B at a grade of 17.99 wt.% and 7.27 wt.% U_3O_8 respectively (Denison, 2010). In zones A and B, the mineralization is mostly pitchblende, with anomalous amounts of copper (up to 3,100 ppm Cu) and lead (up to 9.83 wt % Pb), and minor nickel (up to 461 ppm Ni), cobalt (up to 119 ppm Co), arsenic (up to 170 ppm As), zinc (up to 1,070 ppm Zn) and silver (up to 0.1 ppm Ag) (Kerr, 2011; this study). The ore is proximal to the unconformity between the early Paleoproterozoic crystalline basement rocks and the overlying Read Formation quartzarenite, breccia, conglomerate and pebbly quartzarenite, approximately 400 m beneath the present day surface. The ore bodies are located within or near graphitic pelite of the Wollaston Supergroup, and are elongated and narrow, approximately 25-50 m in width. The WS shear, the main structural feature associated with this deposit, is a NE-SW trending (055° azimuth) reverse fault that dips 55° to the SE at the base of the graphitic pelite along the footwall of the quartzite ridge (Arseneau and Revering, 2010). The closely associated WS hanging wall shear, to the east of the ore zones, is thought to have been the main conduit for the mineralizing fluids along with the WS shear (Arseneau and Revering, 2010). Both shear zones are well defined in the basement rocks, but split into splays that become diffuse and tend toward parallelism with bedding in the overlying siliciclastic units. Therefore, these shear zones are very difficult to trace within the Athabasca Group.

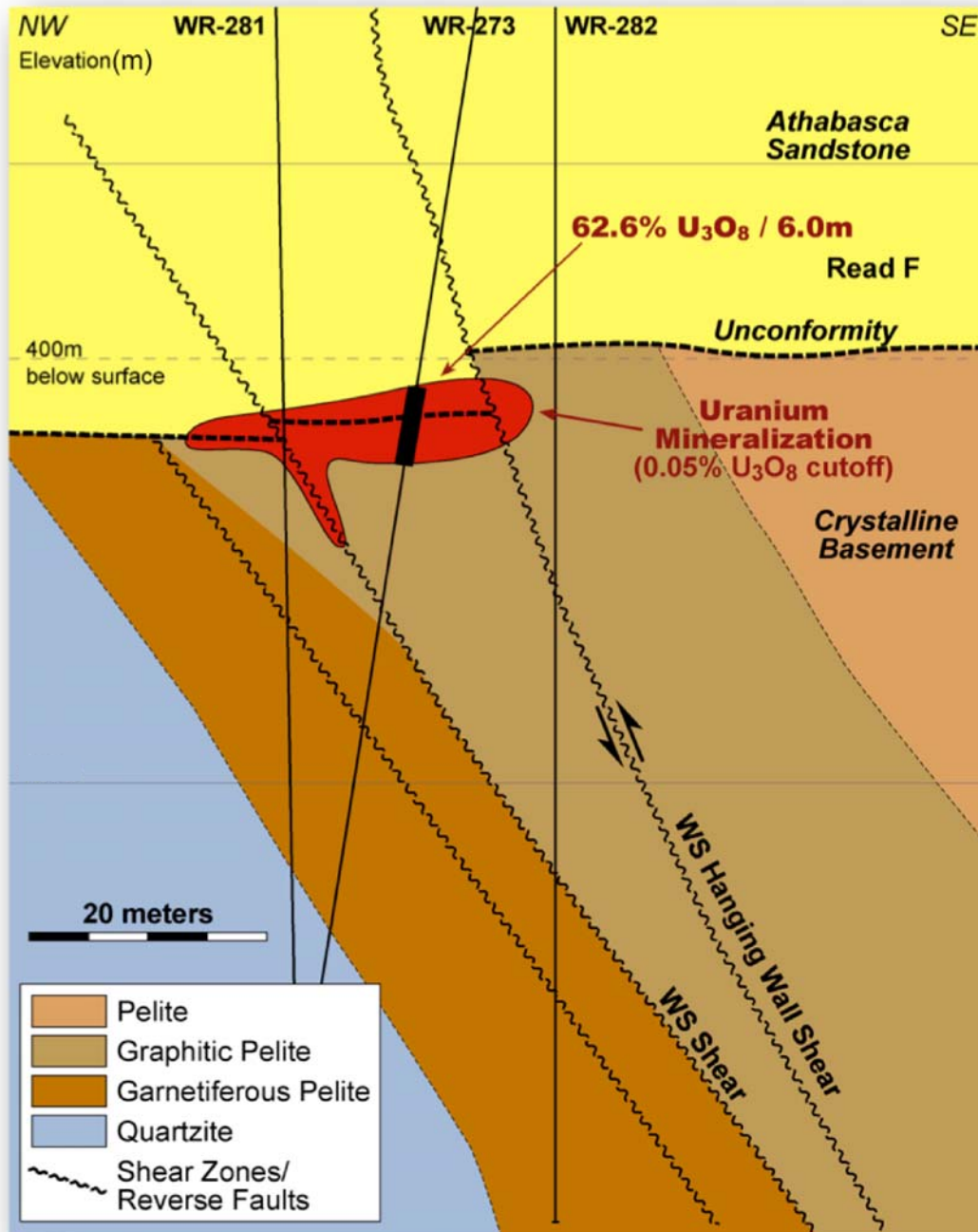


Figure 2: Schematic cross section of the Phoenix deposit from Gamelin et al., (2010).

As reported by Kerr (2011) alteration mineralogy in the overlying Athabasca Group is typical of Athabasca unconformity-related uranium mineralization: varying silicification and de-silicification, dravite, chlorite, illite, kaolinite, hematite and drusy quartz (*cf.* Jefferson et al., 2007). Of note, the property lies along the northeast-trending, regional illite trend defined by Earle and Sopuck (1989) which envelopes the Key Lake, Millennium and McArthur River deposits. Alteration in the basement pelite and graphitic pelite consists of strong bleaching and intense chlorite and illite replacement (Kerr, 2011).

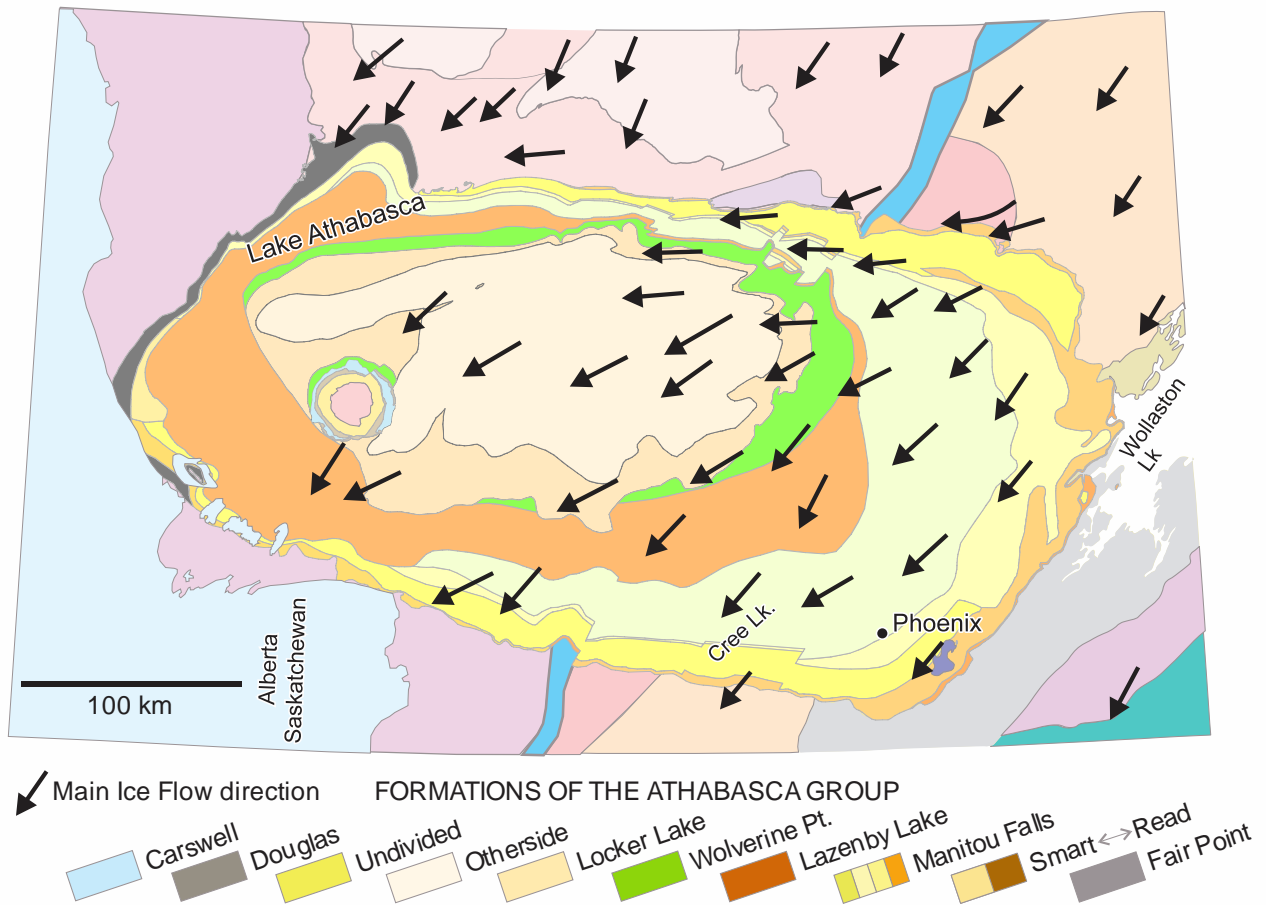


Figure 3: Regional ice flow pattern of the last glacial event approximately 10,000 years ago in Northern Saskatchewan; the dominant ice flow direction is shown by the black arrows (modified from Campbell, 2007).

Topography

The area has experienced several glacial events involving multiple ice flow directions and reworking. The most dominant late ice flow direction (Fig. 3) was southwesterly as deduced from the morphology of the largest drumlins, although these were weakly overprinted by later more west-southwesterly ice flow (Campbell, 2007). The surface topography consists mainly of gently rolling hills of glacial deposits consisting of eskers, outwash sand plains, drumlins, till plains and glaciofluvial plain deposits (Fig. 4) (Campbell, 2007), which border the deposit to the northwest and southeast; this is typical of the “taiga” forestland emblematic to the Basin area. The taiga in the study area is more than 90% young jack pine in the order of 2 to 3 m tall (Fig. 5) with rare older stands up to 5-10 m high. The jack pine is regularly subject to extensive natural forest fires that open its cones for regeneration. Black spruce is limited to the fringes of water bodies and low boggy areas. Minor local stands of white birch are found in some well-drained areas. The trees are set in a thin carpet of caribou moss (lichen) with local clumps of shrubs. Glacial till on the property is generally 25 m thick (most sample sites of this study), but reaches more than 100 m in places.

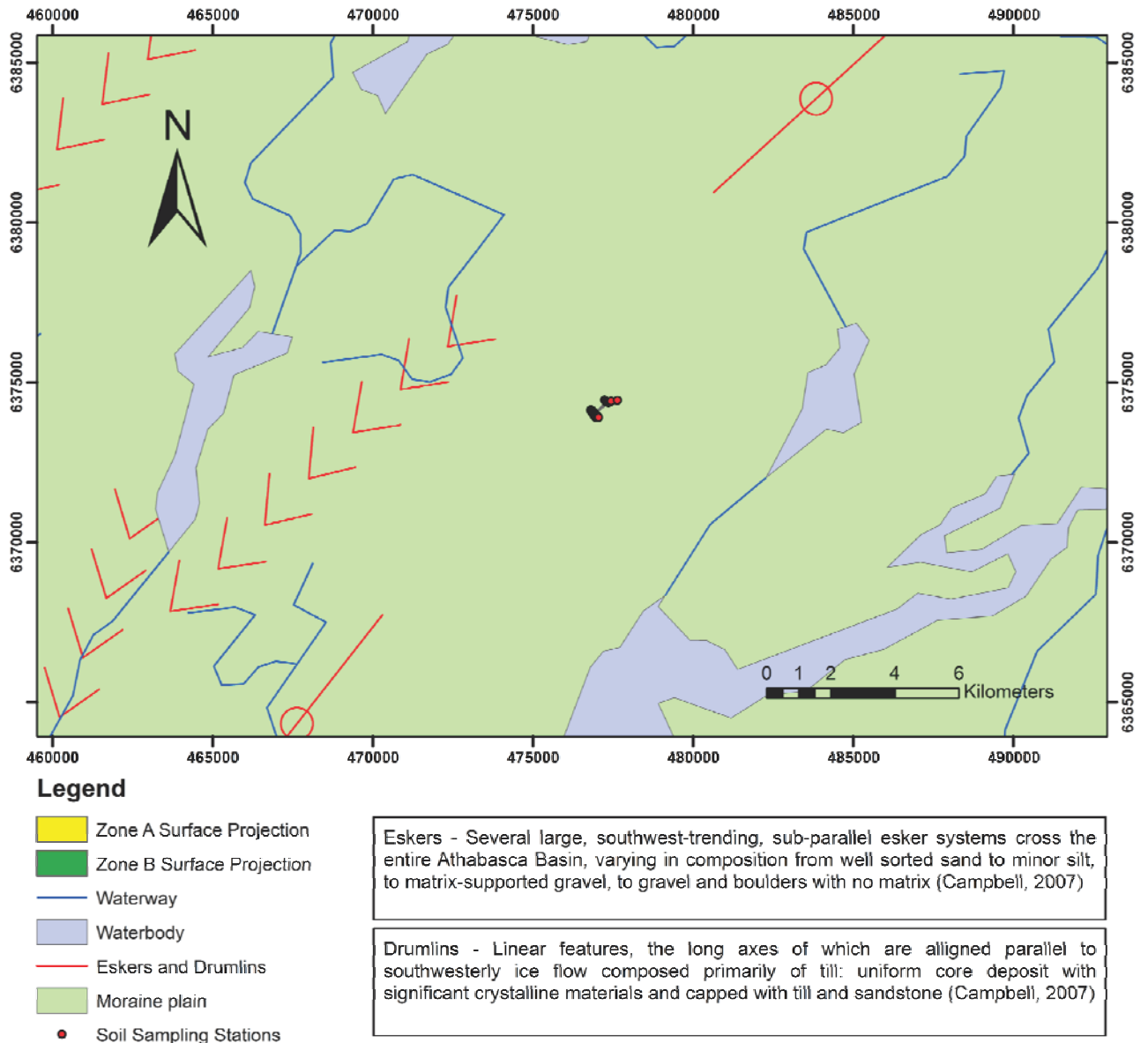


Figure 4: Property scale (approximately 1:60,000 scale) surficial geology map at Wheeler River (modified from Schreiner, 1984) with soil sampling stations and ore zone surface projections (shown in middle). The Phoenix deposit is situated in an area of glacial moraine plain. Southwest-trending eskers and drumlin are symbolized by sinuous herringbone patterns and drumlins by lines through open circles.



Figure 5: Typical northeast-looking view of the study area showing a mineral lease access road cutting gently rolling hills covered in 2-3 m high jack pine trees and black spruce (dark lines in distant low ground). Note relict black trunk of recently burned jack pine in lower right. Photograph taken in September, 2011.

Climate

The research area has a sub-arctic climate with long, cold winters followed by warm, wet summers, and approximately 475 mm of annual precipitation (Canadian Plains Research Centre, University of Regina, 2007). The area lies in a region of sporadic discontinuous permafrost (Burgess et al., 1999).

Soil Conditions

At most sampling stations, well developed soil horizons are present (Fig. 6). The humus (A1 horizon) is thin (0-5 cm), relatively dry and very dark, indicating a high content of organic matter. Horizon E (5-10 cm) is sandy, greyish-white and the boundary with the overlying humus is gradational in many places. The B horizon ranges in thickness from 10 to 30 cm, is yellowish-brown in color, and has a well-defined contact with the overlying E-horizon. The C-horizon, essentially fresh glacial till deeper than 30 cm, comprises cream coloured silt and sand with very minor clay.



Figure 6: (left) Typical soil horizon profile. The humus layer includes charcoal from a previous forest fire event. The photo was taken at 57° 30' 32.285" N, 105° 23' 10.768" W. (Right): Representative soil sample from station PHX-041.

Sampling Methods

Samples for this scoping study were collected along linear transects over ore zones rather than on grid or composite patterns. The transects facilitated sampling “background values” at stations far away from the ore zones in the specific soil environments being studied. Three transects were selected, with 10 m sampling intervals dictated by the narrow aspect of the ore bodies. The soils and vegetation over Zone A had been disturbed by drilling-related activity, so only one transect along the northern edge of the zone was possible. However, the surface media overlying Zone B were less disturbed, allowing for 2 transects over the ore zone. Sampling along each transect was completed over a one to two day period using a Dutch auger and trowel. Transect A, consisting of 22 sampling locations, was completed from the northwest to southeast across the northern extension of Zone A, whereas Transects B and C, consisting of 19 and 18 sampling stations, respectively, were completed from the northeast to southwest across Zone B. One station, PHX 022, was taken approximately 200 m to the northeast from PHX 021 to serve as background to any possible anomalies found overlying Ore Zone A.

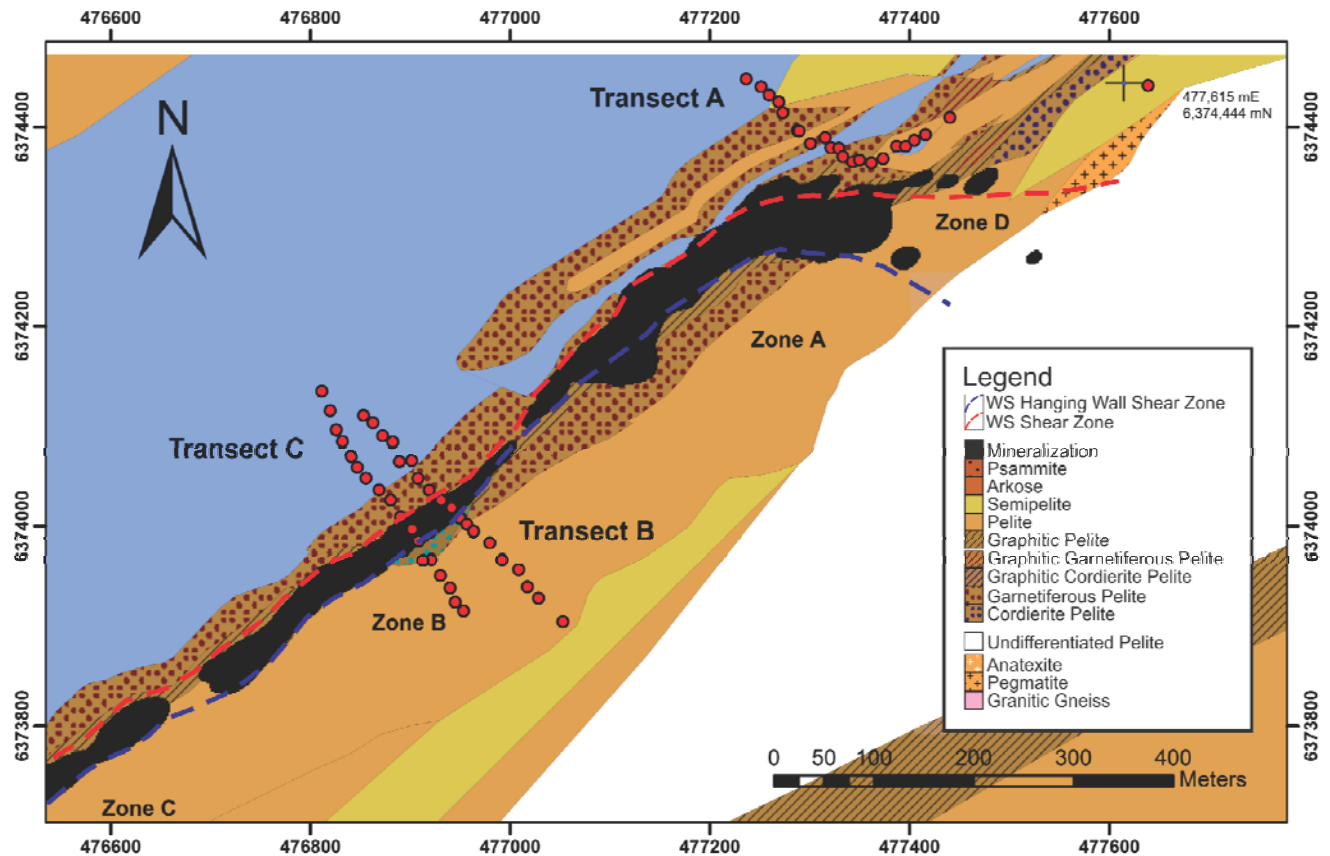


Figure 7: Soil sampling stations (solid red circles) along three transects plotted on Denison Mines Corp's basement geology map of Zones A through D of the Phoenix deposit, with the WS and WS Hanging Wall shear zones bounding it to the west and east, respectively. Two transects were sampled over Zone B because the area above it is not disturbed, unlike the area above the Zone A. The sample sites are approximately 10 metres apart.

A total of 226 soil samples (humus, B, E, and C horizon) (Fig. 7) from 59 sites along 3 transects over Zones A and B were collected approximately 10 metres apart in undisturbed forest. The pH and conductivity were measured in a slurry of soil and distilled water shortly after sampling using a ExStik pH/ORP Meter for pH and Combo PH/EC/TDS/Temperature meter for electric conductivity.

Analytical Methods

Leaches and Digestion

Humus samples were digested by aqua regia after sieving and drying at 60° C, whereas B horizon soil samples were leached by both ammonia acetate (pH 5) and hydroxylamine after sieving and drying. All resulting fractions of both horizons were analyzed by ICP-MS at Acme Analytical Labs in Vancouver, BC (analytical detection limits in appendix). Acetate and hydroxylamine leaches extract elements adsorbed on mineral surfaces or incorporated in secondary calcite and Fe-Mn-O-OH phases (Dalrymple et al., 2005). Duplicate samples were given different sample numbers from those collected along each transect and were used to ensure quality control during the analytical procedures. The whole rock geochemical compositions of sandstone samples collected from drill cores were provided by Denison Mines Corp., who had collected these rock samples at 10 m intervals and

submitted them to the Saskatchewan Research Council (SRC) laboratories for near-total digestion with HF-HNO₃-HCl and analysis by ICP-MS and ICP-OES methods.

Mapping Software

The spatial distributions of soil and sandstone data were analyzed using the ArcMap™ function of the ESRI ArcGIS™ software platform. The sandstone data were further interpolated element-by-element by the inverse weighted distance (IDW) method to determine unknown values based on proximity to known values in a defined neighborhood. This method is effective for dense data populations (de Smith et al., 2008). It calculates the weighted mean of known values inside a moving window and assigns this value to the central pixel of a polygon. All interpolated values are between the minimum and maximum observed values of the total sample population. The sandstone maps showing interpolated element abundances were used as an independent base on which the soil transect results for the various leaches were plotted (Figures 11 to 21 inclusive). The ore zones A and B are also outlined for reference

Results

The humus results (Fig. 8) show significant variations in the concentrations of U and Co, Ni, Mo, Ag and W. Among these metals, Co and Ni are considered to be pathfinder elements for uranium deposits in surface media in the region (Jefferson et al., 2007b). All these elements are anomalous at sites along the transects overlying the surface traces of the ore zones, but are also anomalous above where the WS hanging wall shear zone is thought to extend upward from the basement through the sandstone to the surface.

Peak to background ratios of element concentrations are up to 6 for uranium (5.7 ppm U), 5 for molybdenum (4.8 ppm Mo), 4 for cobalt (5.2 ppm Co), 20 for silver (0.98 ppm Ag) and 18 for tungsten (100 ppm W) in the humus. In both the A and C transects uranium concentrations peak above the basement shear zone. Molybdenum is anomalous above Zone B along transect B and above the WS hanging wall shear zone adjacent to the surface projection of the ore zone in Transects A and C. Cobalt concentrations are anomalous in the area above the shear zone in Transect A and C, as well in on the B ore trace in Transect B. Sharp tungsten anomalies, with respect to background, are also located above the shear zone in Transect A, and on the ore trace in Transect B.

Results were also plotted as ratios to aluminum and iron which are interpreted as relatively immobile in the soil environment, and therefore normalize the data. Both aluminum and iron contents are very low in organic-rich samples but high in the underlying E-horizon soil. Therefore, aluminum and iron can be used to monitor the possible contamination from nearby drilling activity. In addition, aluminum and iron are most likely endogenic in the soil and the ratios enhance the amounts of exogenic elements. For both the molybdenum/aluminum and silver/iron ratios, anomalies are very strong in the shear zone in Transects A and C, and over the ore trace on Transect B.

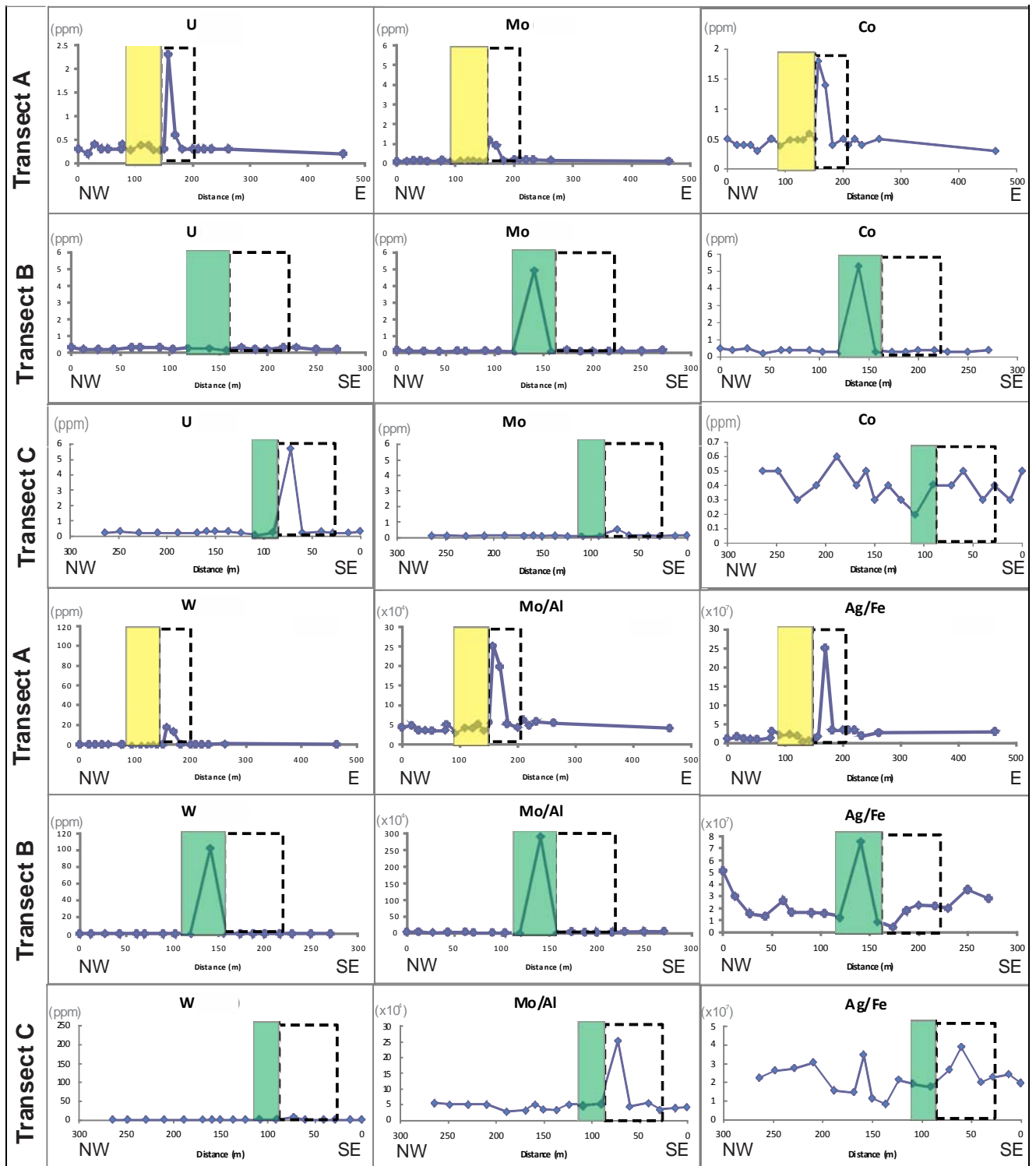


Figure 8: Element abundances along the transects: U, Mo, Co, W and weight ratios of Mo/Al and Ag/Fe in humus. The yellow box indicates the area directly above Zone A, green the area above Zone B, and the dotted rectangle encompasses the likely surface projection of the diffuse WS Hanging Wall Shear Zone.

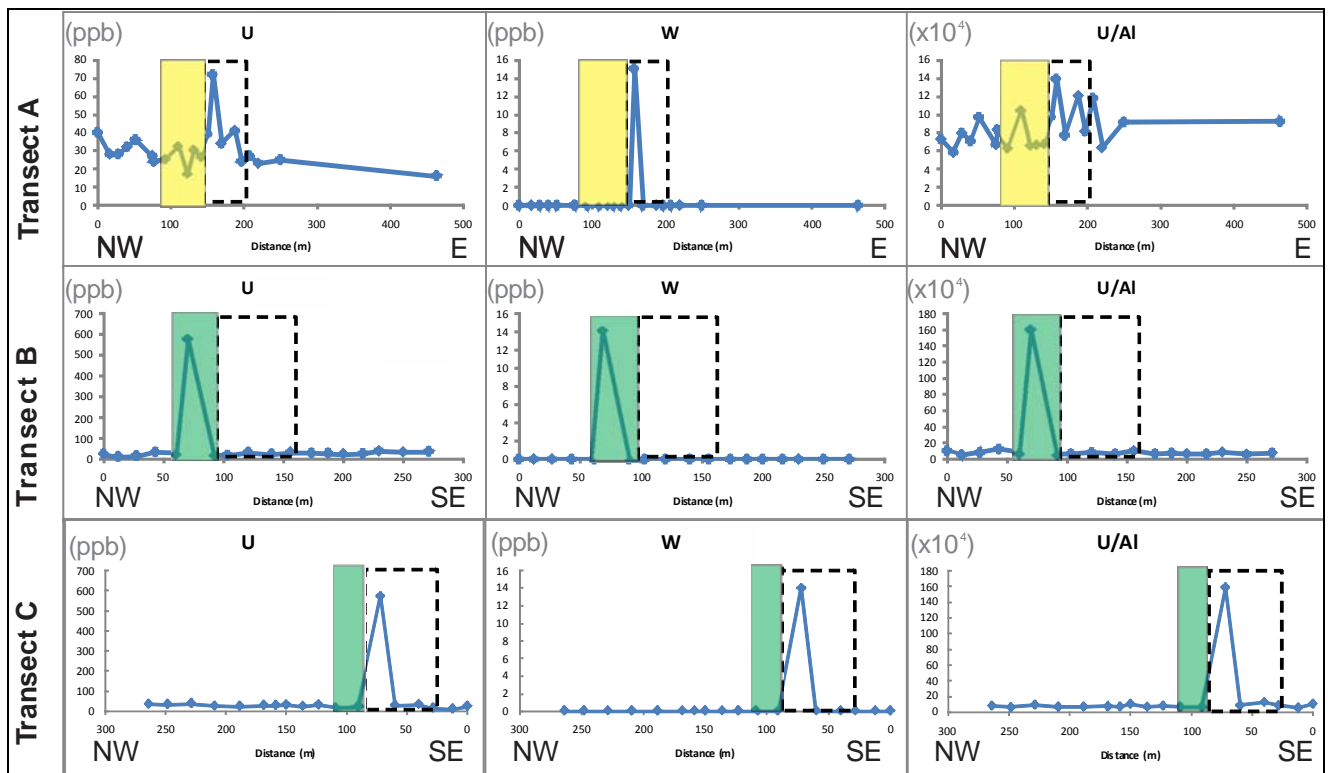


Figure 9: Element abundances along the transects: U, W, and weight ratio of U/Al_2O_3 in ammonium acetate pH 5(AA5) leach of B-horizon soil. Ore and fault zones denoted as in Figure 8.

Although the absolute concentrations of U, W and Ag in both leaches of the B horizon soil samples are an order of magnitude less than those in the humus, these elements display anomalous values with respect to the background levels determined by this study. Peak to background ratios of element concentrations are up to 10 for uranium (with maximum concentration of 573 ppb U), 1.5 for silver (11 ppb Ag) and 16 for tungsten (16 ppb W) in this horizon. Normalizing these elements to aluminum yields very similar anomalies, demonstrating that they are robust when compared to an immobile element. Anomalies are situated in the surface area directly above the ore zones and directly above the basement location of the WS Hanging Wall shear zone (Figs. 9 and 10).

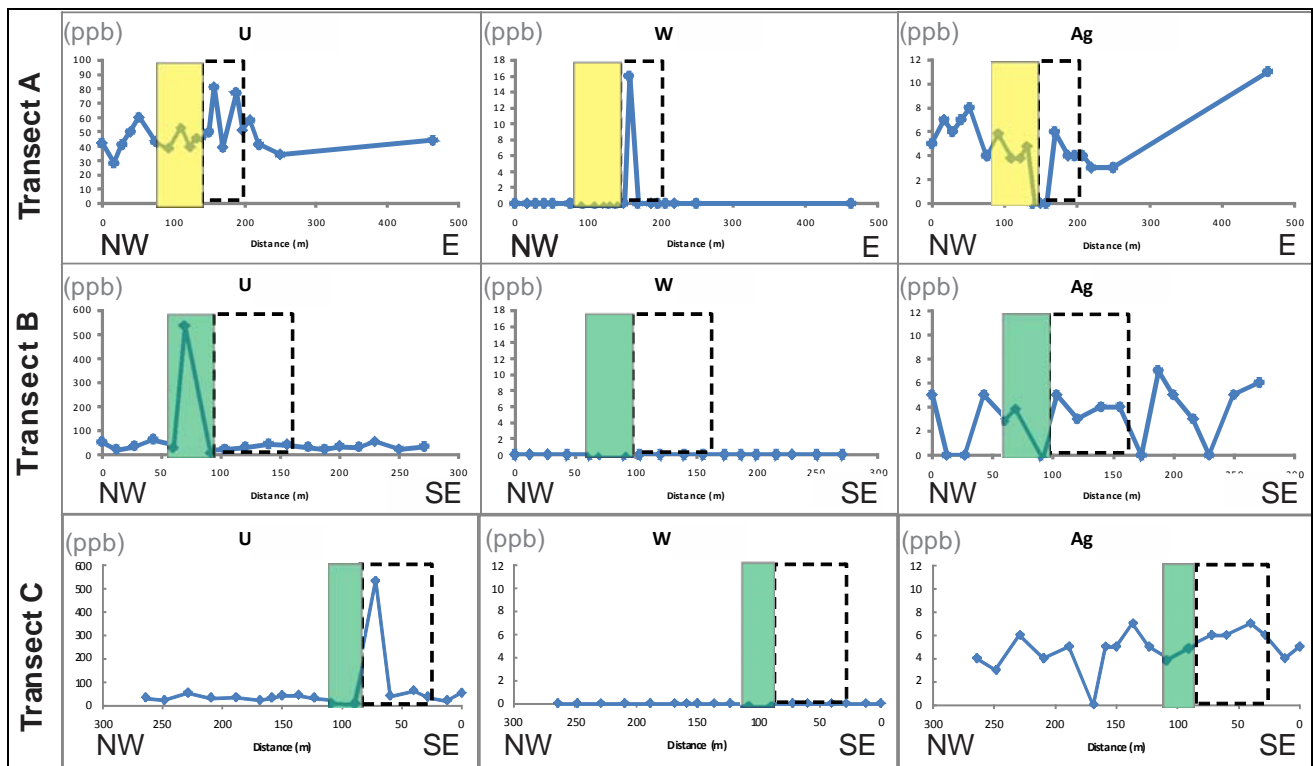


Figure 10: Element abundances along the transects: U, W and Ag in B-horizon soil after hydroxylamine leach. Ore and fault zones denoted as in Figure 8.

As noted above, raster maps of the interpolated sandstone element abundances from the uppermost drill hole lithochemical data (Figs. 11 - 22) are provided as an independent underlying data context for the soil geochemical data. Uranium in sandstone is anomalous along the trace of Zone A, as well as along trend immediately SE of both zones (WR-339, WR-260, WR-249), on a similar order of magnitude to the humus data (values of up to 5 ppm for high U). Anomalies in the cobalt raster map are not as widespread but still evident on the southern section of the Zone B trace (WR-260, WR-259, WR-258, WR-262, WR-265) and in a few drill holes SE of Zone A (WR-190A, WR-249, WR267-69) (values up to 1 ppm for high Co). The raster for copper displays a similar anomalous area SW of the Zone B trace (WR-295, WR-260) and south of the Zone A trace (WR-268, WR-272, WR-273, WR-277) (values up to 15 ppm for high Cu). The element raster map for molybdenum (with values up to 1 ppm Mo) shows anomalies very similar to those for cobalt in the same areas SE of the ore zones. The silver and tungsten raster maps also show anomalies in these localities, but the anomalies are more subtle (0.21 ppm and 1 ppm, respectively) than values obtained in humus for the same elements. The raster map for lead conversely shows anomalies southwest of both ore zones although these are limited to three drill holes (WR-339, WR-289 and WR-277).

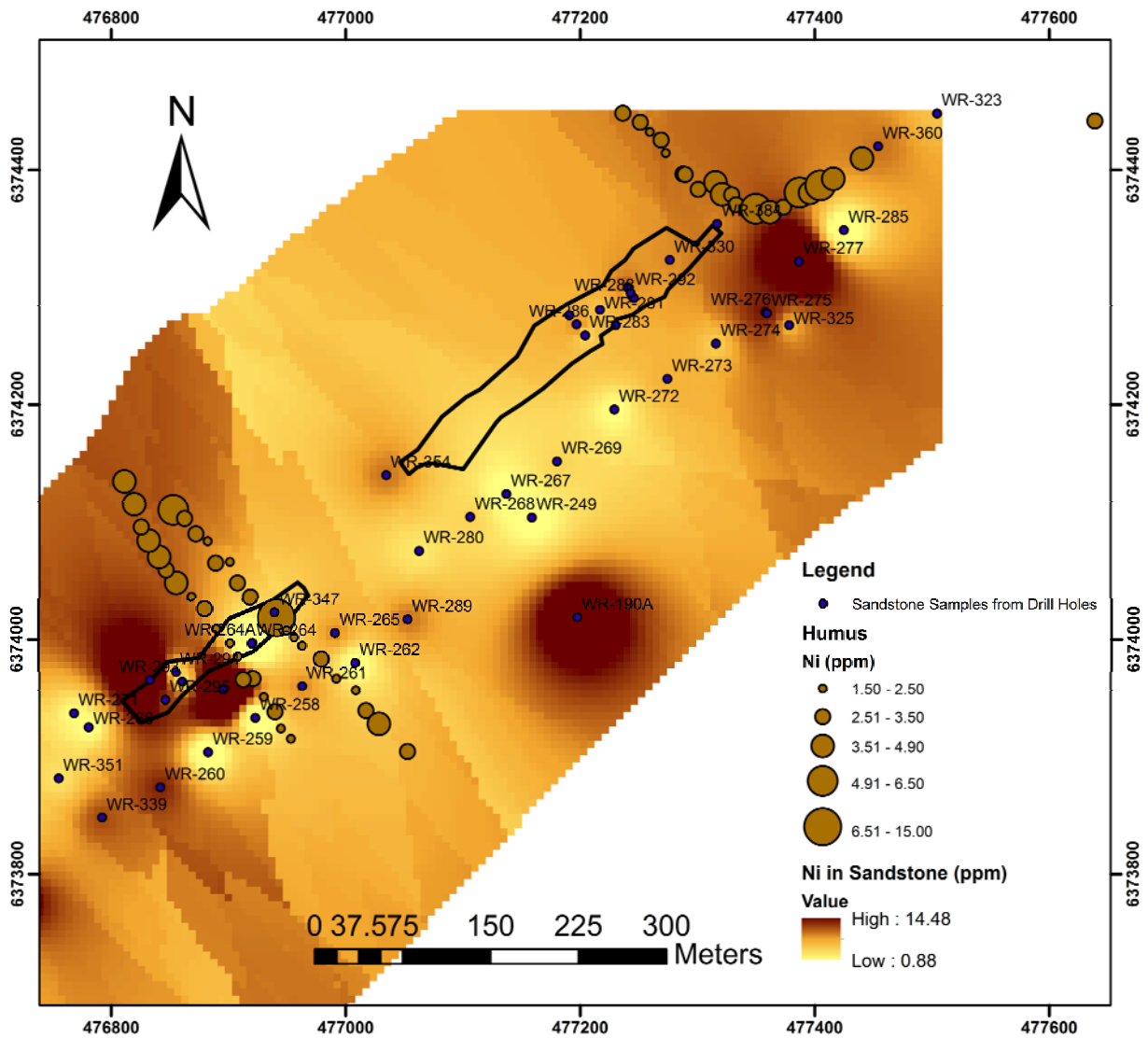


Figure 13: Contoured geochemical results for Ni in humus soil samples and Dunlop Member sandstone. Coordinates are projected in UTM, NAD 83, Zone 13.

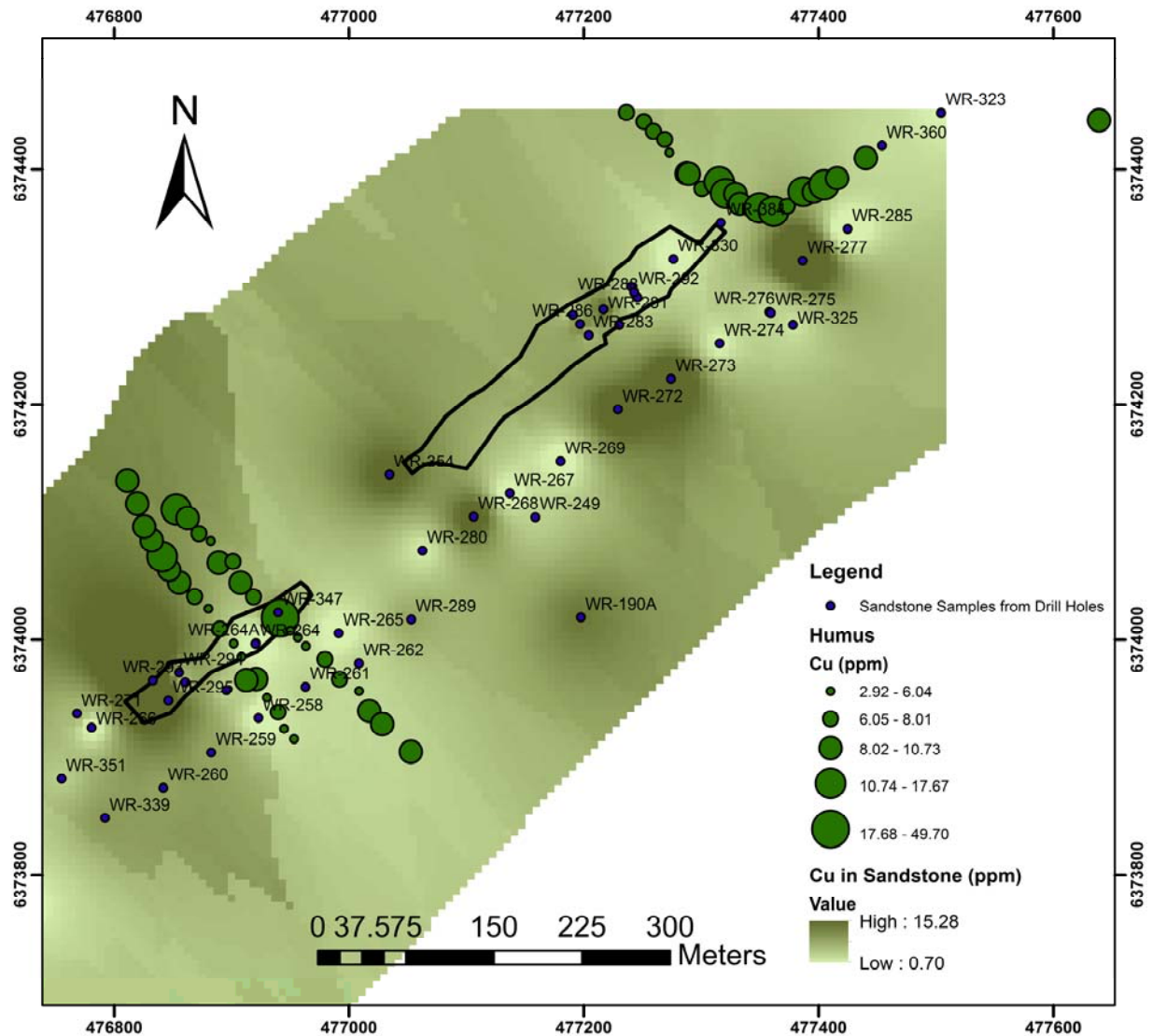


Figure 14: Contoured geochemical results for Cu in humus soil samples and Dunlop Member sandstone. Coordinates are projected in UTM, NAD 83, Zone 13.

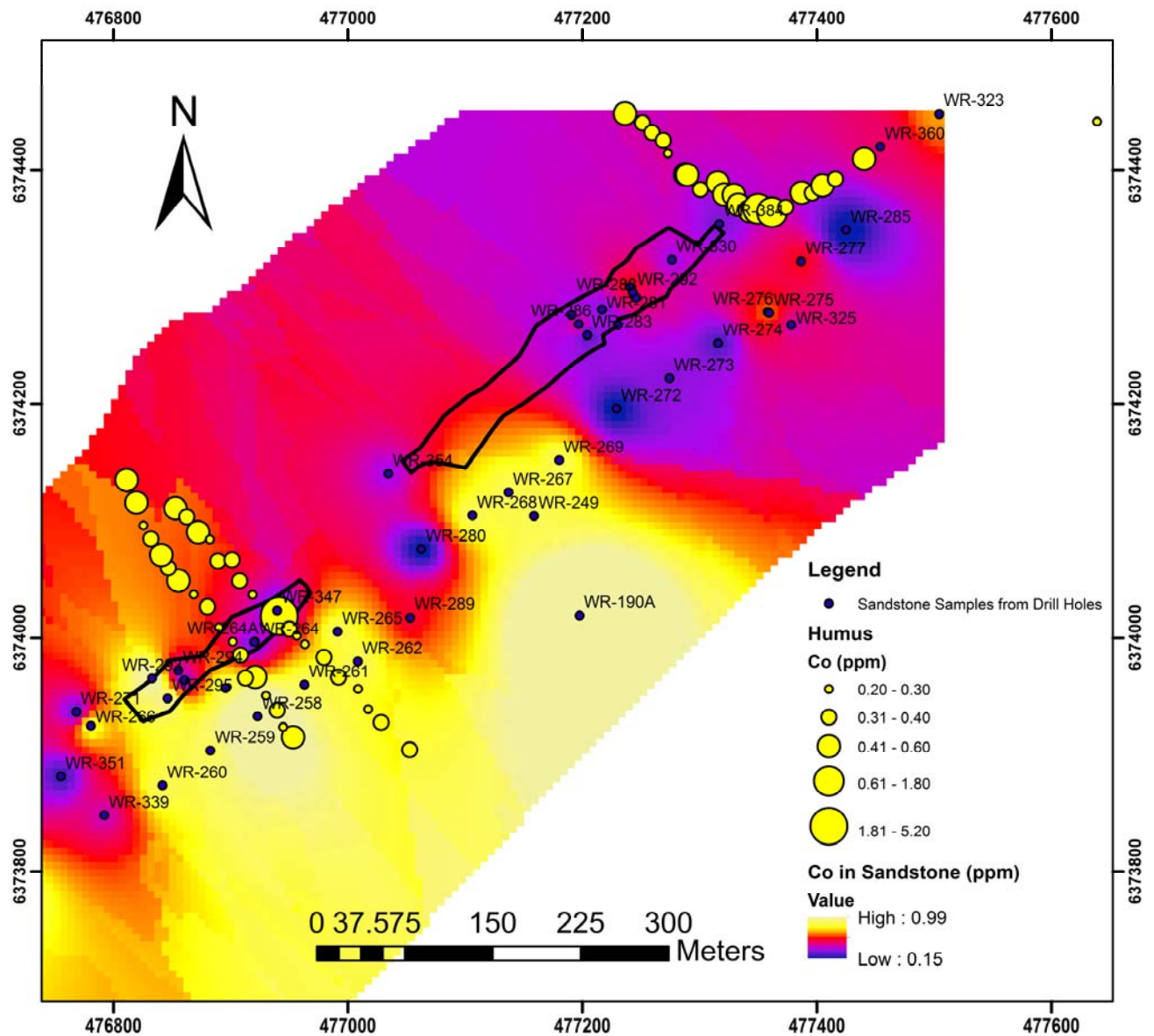


Figure 15: Contoured geochemical results for Co in humus soil samples and Dunlop Member sandstone. Coordinates are projected in UTM, NAD 83, Zone 13.

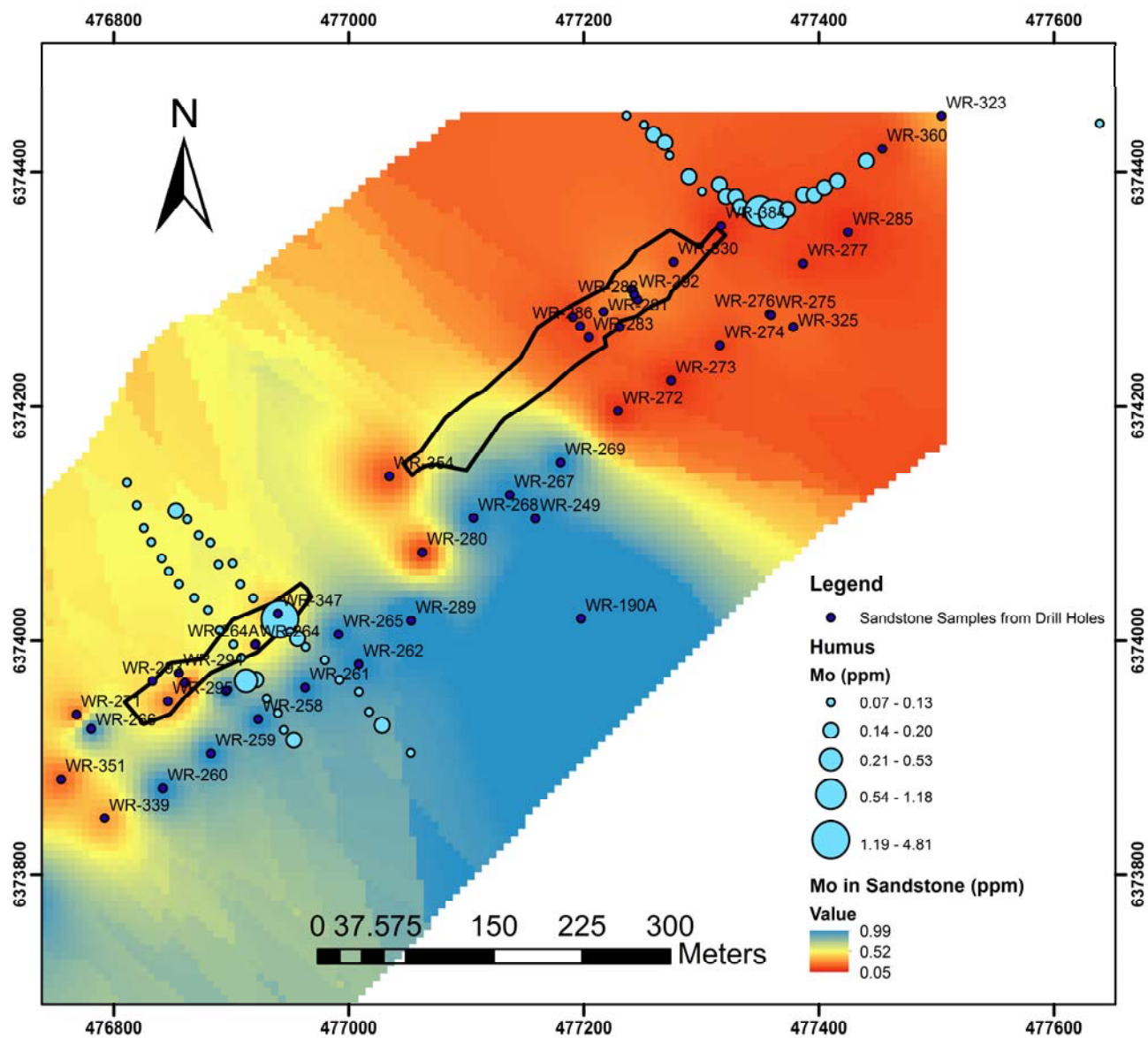


Figure 16: Contoured geochemical results for Mo in humus soil samples and Dunlop Member sandstone. Coordinates are projected in UTM, NAD 83, Zone 13.

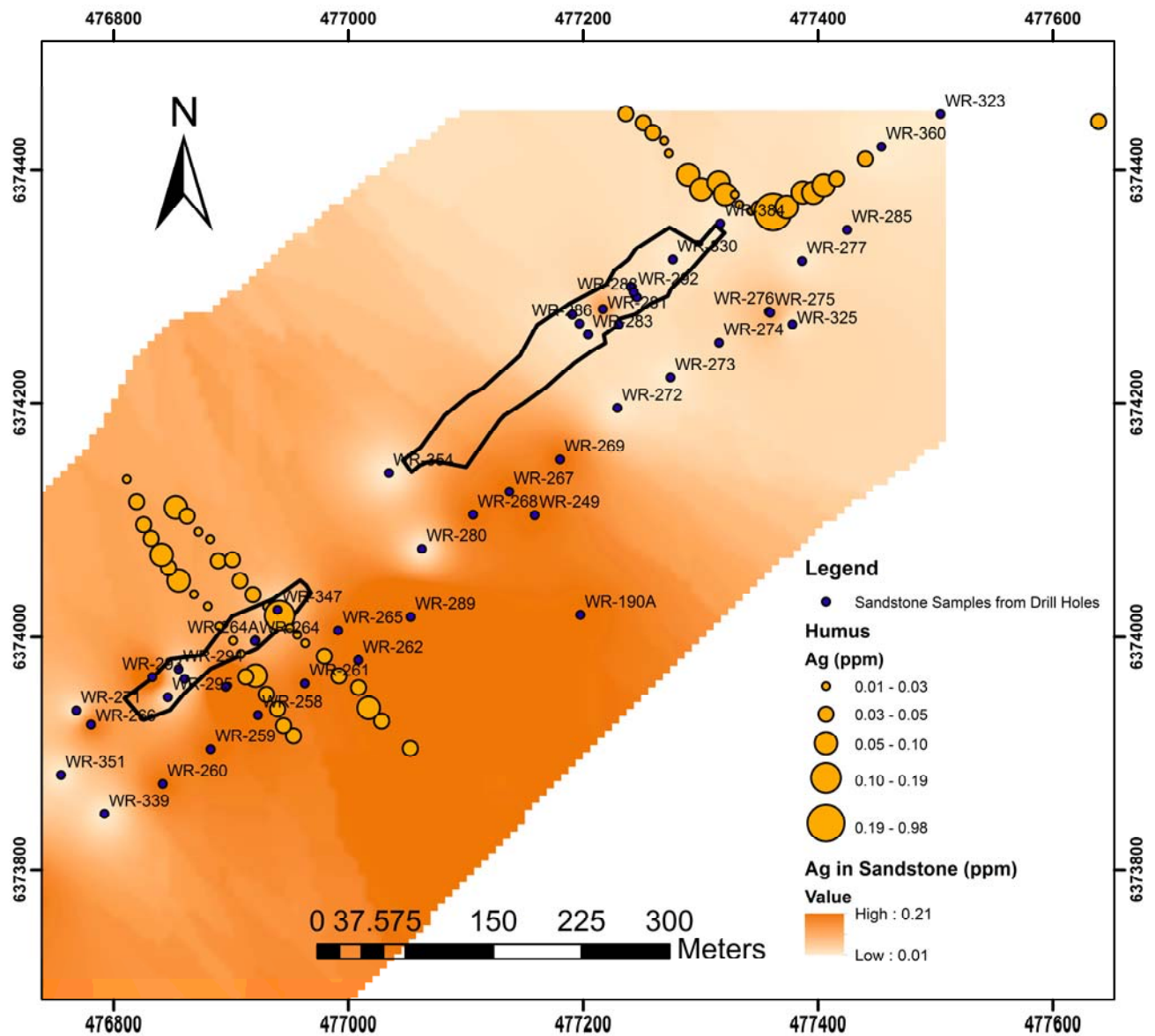


Figure 17: Contoured geochemical results for Ag in humus soil samples and Dunlop Member sandstone. Coordinates are projected in UTM, NAD 83, Zone 13.

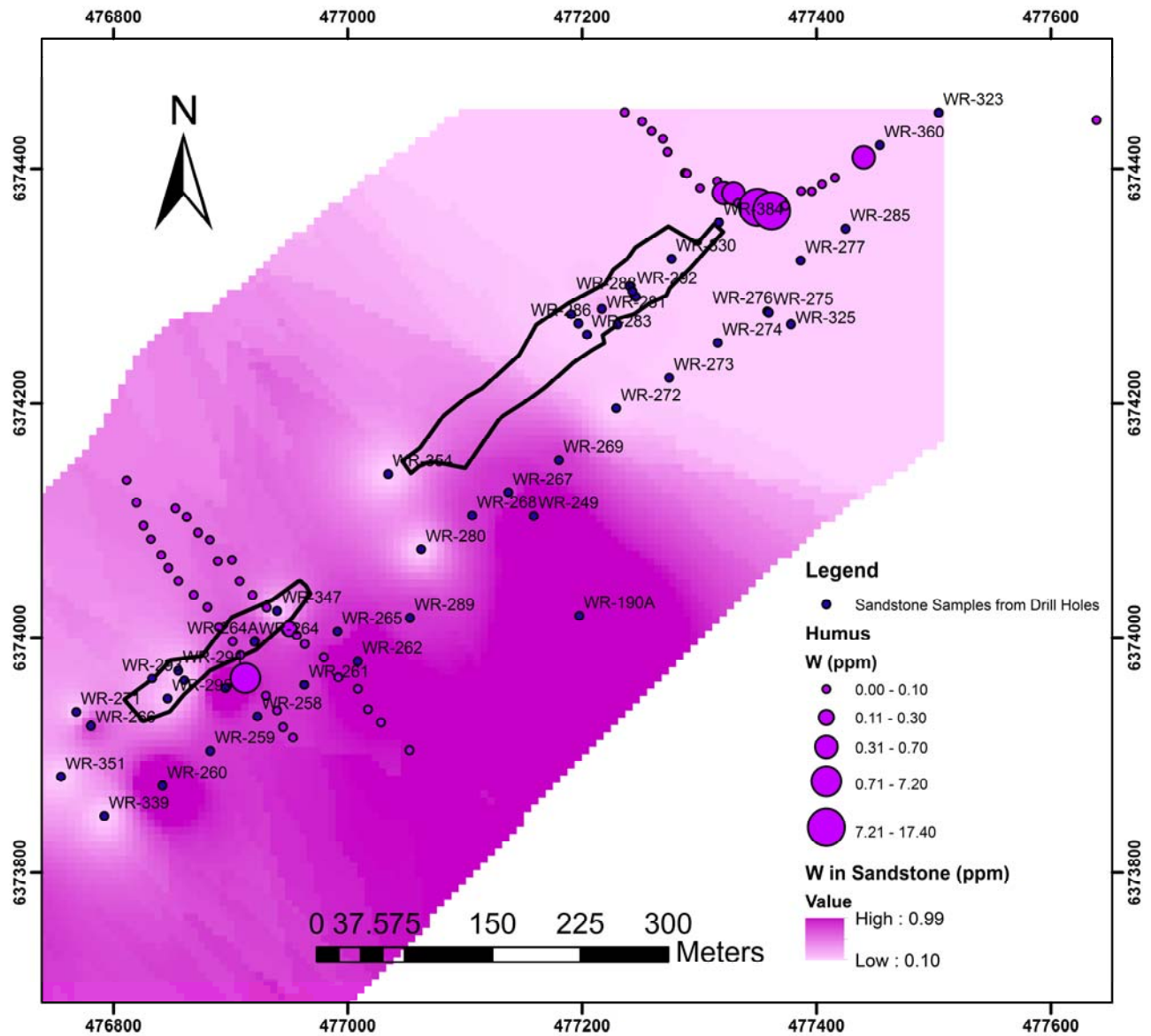


Figure 18: Contoured geochemical results for W in humus soil samples and Dunlop Member sandstone. Coordinates are projected in UTM, NAD 83, Zone 13.

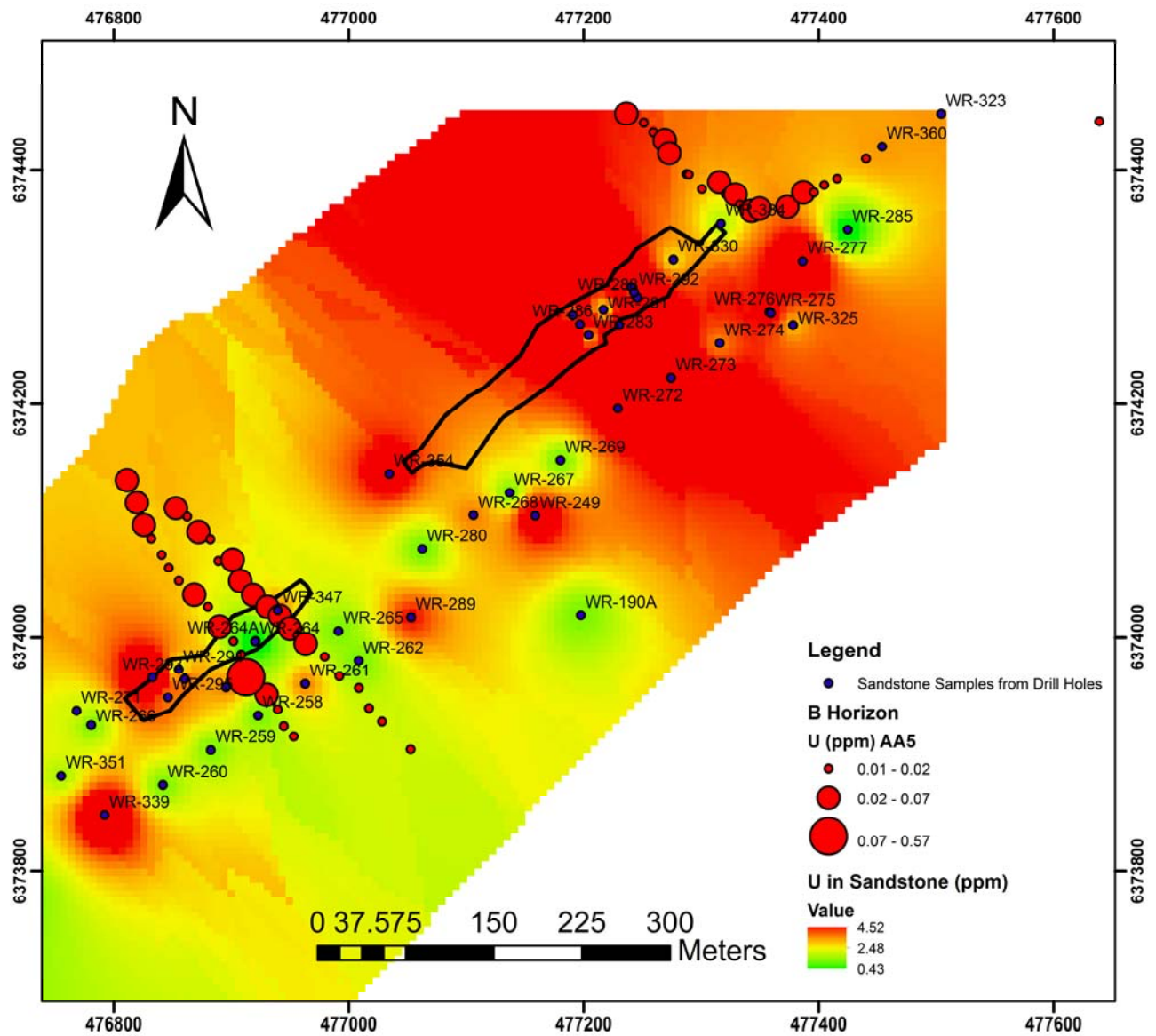


Figure 19: Contoured geochemical results for U in B-horizon soil samples and Dunlop Member sandstone. Coordinates are projected in UTM, NAD 83, Zone 13.

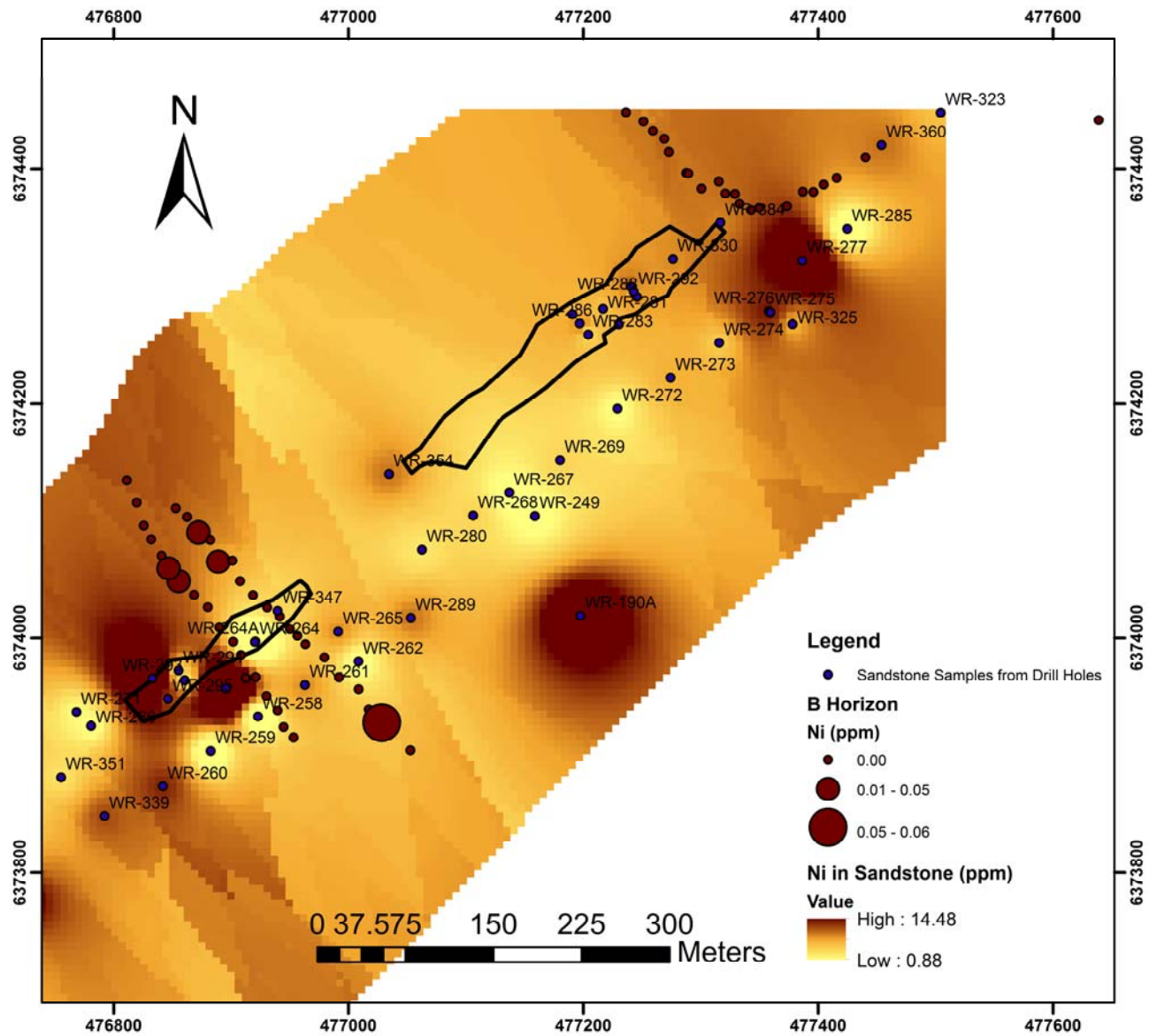


Figure 20: Contoured geochemical results for Ni in B-horizon soil samples and Dunlop Member sandstone. Coordinates are projected in UTM, NAD 83, Zone 13.

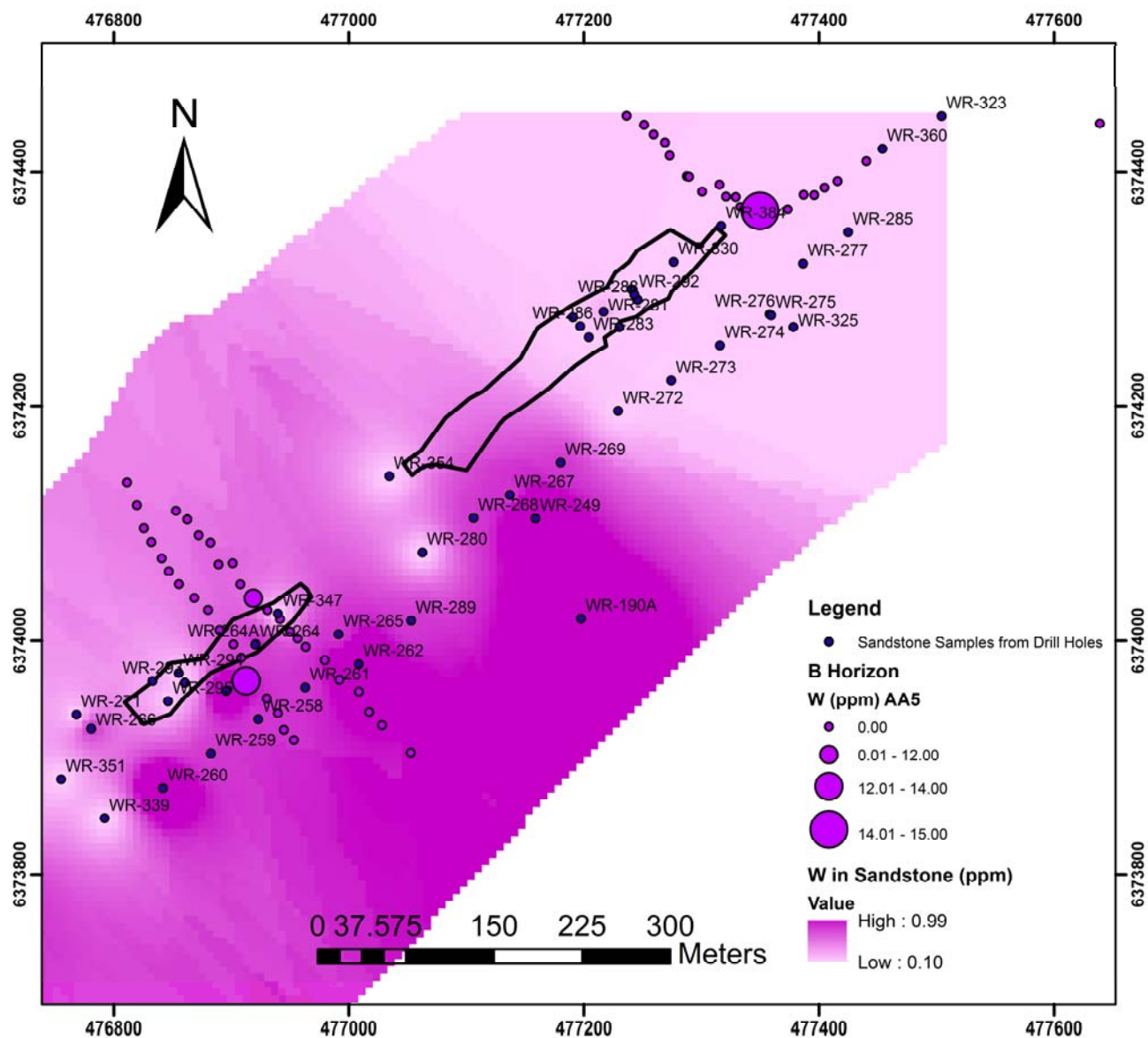


Figure 21: Contoured geochemical results for W in B-horizon soil samples and Dunlop Member sandstone. Coordinates are projected in UTM, NAD 83, Zone 13.

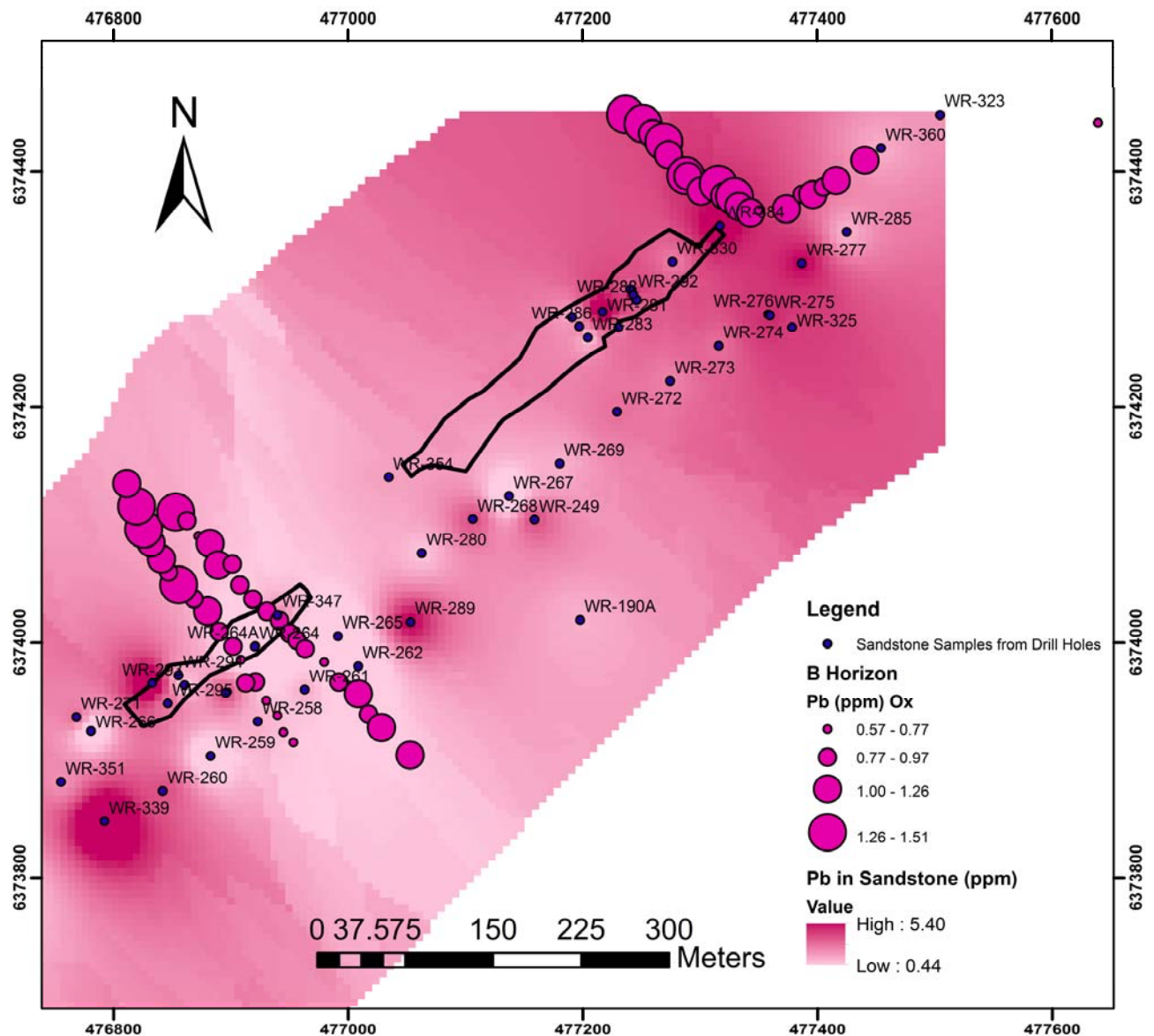


Figure 22: Contoured geochemical results for Pb in B-horizon soil samples and Dunlop Member sandstone. Coordinates are projected in UTM, NAD 83, Zone 13.

Although clear soil geochemical anomalies directly overlie the Phoenix ore zones, no anomalies are observed directly over the basement location of the WS Hanging Wall shear zone mineralization. The southeast dipping (55°) shear zone should project at surface almost 300 m northwest of the ore zone, and follow up geochemical sampling will focus on this location. However, the shear zone most likely splays into several faults within the sandstone and their surface projections should be closer to the ore zone because the shear zone is not observed in drill core of the WR-281 hole. Moreover, it is known that hanging wall splays are associated with the main WS Shear and the fault was likely reactivated after the sedimentation of Athabasca sandstone (Arseneau and Revering, 2010). Furthermore, thinning of Read Formation and Bird Member siliciclastic units over the quartzite ridge and the presence of the quartzite breccia likely indicates pre-, syn- and post-deposition movement along the reverse faults that border the quartzite ridge to the west (Jefferson et al., 2007a, b; Kerr, 2011).

Initial geochemical analyses of the silt fraction of selected C horizon till samples display values of Na_2O more associated with basement granite than with siliciclastic rocks (1-2 wt. % Na_2O). For example, the Dunlop member has virtually no Na_2O .

Discussion

Correlations between soil horizons and uppermost siliciclastic units

The results show that anomalies in uranium and its respective pathfinder elements occur in humus, B horizon over the uranium pods, as well as the area over the WS Hanging Wall shear zone in the basement rocks. There may also be movement of these elements in an east-west trending shear zone that crosscuts the ore zones, as the WS Hanging Wall Shear likely splays out in the siliciclastic units somewhere between where drill holes WR-273 and WR-281 are located (Fig. 2). The plot for U (Fig. 11) shows a good spatial correlation between the geochemical anomalies in soil and the upper sandstone. It is especially evident in the region immediately northeast of Zone B and immediately southwest of Zone A.

The geochemical results from the uppermost Dunlop member siliciclastic units highlight that similar elements of interest in the humus and B soil horizons occur in anomalously high concentrations in regions directly below the soil sampling locations, which suggests that the anomalies in soil reflect those in the siliciclastic rock units. Furthermore, basement shear zones and their splays projected through the Athabasca sandstone likely provided conduits for the upward-transport of elements from the ore zones to the surface.

Transport mechanisms of elements from concealed mineral deposits to surface media have been in debate (*cf* Cameron et al., 2004, Leybourne and Cameron, 2010). Proposed hypotheses include electrochemical transport of ions (Hamilton et al., 2008), upwelling of groundwaters (Sader et al., 2011), ground and soil water advectations or diffusion (Govett, 1976), vapour transport (Smee, 1998), seismic pumping (Cameron et al., 2002) and capillary migration of ions (Mann et al., 2005). Planned sampling of ground waters and gases may provide more information on the dominant processes occurring at Wheeler River. However, as noted by Alexandre et al., (2009) the numerous U-Pb isotopic re-setting events recorded in most of the Athabasca basin uranium deposits (e.g. 1.5.-1.6 Ga, 1.4 Ga, 1.27 Ga, 1.0 Ga and 0.85 Ga) coincide with continent-wide tectonic events such as the Masatzal orogeny, Berthoud orogeny, intrusion of MacKenzie mafic dykes, Grenville orogeny and assembly and break-up of Rodinia, respectively. These relationships likely reflect the role of tectonic-driven seismic pumping in the upward migration of elements from the ore bodies.

Implications for uranium exploration

Surficial geochemical surveys have been proven to be an efficient and inexpensive exploration tool in detecting shallowly buried deposits (*cf* Cameron et al., 2004). This study overlying the Phoenix deposit that lies 400 m beneath the surficial geochemical media shows that such analysis is also capable of detecting deeply buried deposits, even in discontinuous permafrost regions of Canada, where the dispersion of metals is slow at low temperatures and may not exist in frozen ground. In addition, this study confirms that geochemical analysis of shallow siliciclastic rock units likely provides additional valuable information related to the presence of a buried deposit at deep levels.

Acknowledgments

Denison Mines Corp. provided much valuable information on the Wheeler River property including maps and drill core data, as well as logistical support for field work in September, 2011. The project was supported by the TGI4 Program of the Geological Survey of Canada, Natural Resources Canada. We thank Cathryn Bjerkelund of the Geological Survey of Canada for guiding our application and administering the award of the TGI4 grant. The senior author also was supported by a bursary from TGI4 through the Government of Canada's Research Affiliate Program.

References

- Alexandre, P., Kyser, K.T., Thomas, D., Polito, P and Marlat, J., 2009. Geochronology of unconformity-related uranium deposits in the Athabasca Basin, Saskatchewan, Canada and the integration in the evolution of the basin; *Mineralium Deposita*, Vol. 44, p. 41-59.
- Arseneau, G. and Revering, C., 2010. Technical Report on the Phoenix Deposit (Zones A & B) – Wheeler River Project, Eastern Athabasca Basin, Northern Saskatchewan, Canada; NI 43-101 Technical Report prepared for Denison Mines Corp., 2010.
- Bosman, S.A. and Korness, J., 2007. Building Athabasca Stratigraphy; Revising, Redefining, and Repositioning, In Summary of Investigations, 2007, Volume 2; Saskatchewan Geological Survey, Saskatchewan Ministry of Energy and Resources, Misc. Rep. 2007-4.2, CD-ROM, Paper A-8, 29 p.
- Burgess, M., Brown, R., Duguay, C., Nixon, M., Smith, S., Wright, F., 1999. Canadian Contributions to GCOS - Permafrost: a background document to assist in the development of a Canadian initial observing system for the Global Climate Observing System, 23 p.
- Cameron, E.M., Hamilton, S.M., Leybourne, M.I., Hall, G.E.M., McClenaghan, M.B., 2004. Finding deeply buried deposits using geochemistry; *Geochemistry: Exploration, Environments and Analysis*. Vol. 4, p. 7-32.
- Cameron, E.M., Leybourne, M.I. & Kelley, D.L. 2002. Exploring for deeply covered mineral deposits: Formation of geochemical anomalies in northern Chile by earthquake-induced surface flooding of mineralized groundwaters; *Geology*, 30, p. 1007–1010.
- Campbell, J.E., 2007. Quaternary geology of the eastern Athabasca Basin, Saskatchewan; *In* C.W. Jefferson, and G. Delaney, (eds.), EXTECH IV: Geology and Uranium EXploration TECHnology of the Proterozoic Athabasca Basin, Saskatchewan and Alberta, Geological Survey of Canada Bulletin 588, p. 211-228.
- Creaser, R.A., and Stasiuk, L.D., 2007. Depositional age of the Douglas Formation, northern Saskatchewan, determined by Re-Os geochronology; *In* C.W. Jefferson, and G. Delaney, (eds.), EXTECH IV: Geology and Uranium EXploration TECHnology of the Proterozoic Athabasca Basin, Saskatchewan and Alberta; Geological Survey of Canada Bulletin 588, p. 341-346.
- Dalrymple, I.J., Cohen, D.R., Gatehouse, S.G., 2005. Optimization of partial extraction chemistry for buffered acetate and hydroxylamine leaches; *Geochemistry: Exploration, Environments and Analysis*. Vol.5, p.279-285.
- Earle, S. and Sopuck, V. 1989. Regional litho-geochemistry of the eastern part of the Athabasca basin uranium province; International Atomic Energy Agency Tec-Doc 500, p.263-296.
- Gamelin, C., Sorba, C., and Kerr, W. The Discovery of the Phoenix Deposit: A New High-grade, Athabasca Basin Unconformity-type Uranium Deposit, Saskatchewan, Canada; Saskatchewan Geological Survey Open House 2010 Abstract Volume 17.

- Govett, G.J.S. 1976. Detection of deeply buried and blind sulphide deposits by measurement of H⁺ and conductivity of closely spaced surface soil samples; *Journal of Geochemical Exploration*, Vol.6, p.359–382.
- Hamilton, S.M., Cameron, E.M.C., McClenaghan, M.B. and Hall, G.E.M., 2004. Redox, pH and SP variation over mineralization in thick glacial overburden (II): field investigation at Cross Lake VMS property; *Geochemistry: Exploration, Environment, Analysis*, Vol. 4 p. 45-58.
- Jefferson, C.W., Thomas, D.J., Gandhi, S.S., Ramaekers, P., Delaney, G., Brisbin, D., Cutts, C., Quirt, D., Portella, P., and Olson, R.A., 2007a. Unconformity associated uranium deposits of the Athabasca Basin, Saskatchewan and Alberta; *In* W.D. Goodfellow (ed.), *Mineral Deposits of Canada: a synthesis of major deposit types, district metallogeny, the evolution of the geological provinces and exploration methods*, Geological Association of Canada, Mineral Deposits Division, Special Publication No. 5, 273-305.
- Jefferson, C.W., Thomas, D.J., Quirt, D., Mwenifumbo, C.J., and Brisbin, D., 2007b. Empirical Models for Canadian Unconformity-Associated Uranium Deposits; *In* P. Mikereit (ed.), *Proceedings of Exploration 07: Fifth Decennial International Conference on Mineral Exploration*, p. 741-769.
- Jiricka, D., 2008. The Centennial zone – an atypical unconformity-associated uranium deposit; 17th Annual Calgary Mining Forum, Program with Abstracts, April 14-18, 2008.
- Johnson, D., 2007. Canadian Plains Research Center Mapping Division (website) <http://esask.uregina.ca/entry/hydrology.html>
- Kerr, W.C., 2011. The discovery of the Phoenix deposit: a new high-grade Athabasca Basin unconformity-type uranium deposit, Saskatchewan, Canada; *In* R.J. Goldfarb, E.E. Marsh and T. Monecke (eds.), *The Challenge of Finding New Mineral Resources: Global Metallogeny, Innovative Exploration, and New Discoveries, Volume II: Zinc-Lead, Nickel-Copper-PGE, and Uranium*, Society of Economic Geologists, p. 703-725.
- Leybourne, M.I. and Cameron, E.M., 2010. Groundwater in geochemical exploration; *Geochemistry: Exploration, Environment, Analysis*, Vol. 10, p. 99-118.
- Mann, A.W., Birrell, R.D., Fedikow, M.A.F. and De Souza, H.A.F. 2005. Vertical ionic migration: mechanisms, soil anomalies, and sampling depth for mineral exploration; *Geochemistry: Exploration, Environment, Analysis*, Vol. 5, p. 201–210.
- Ramaekers, P., Jefferson, C.W., Yeo, G.M., Collier, B., Long, D.G.F., Drever, G., McHardy, S., Jiricka, D., Cutts, C., Wheatley, K., Canuneanu, O., Bernier, S., Kupsch, B., and Post, R.T., 2007: Revised geological map and stratigraphy of the Athabasca Group, Saskatchewan and Alberta; *In* C.W. Jefferson and G. Delaney (eds.), *EXTECH IV: Geology and Uranium Exploration Technology of the Proterozoic Athabasca Basin, Saskatchewan and Alberta*; Geological Survey of Canada, Bulletin 588, p. 155-191
- Rainbird, R.H., Stern, R.A., Rayner, N., and Jefferson, C.W., 2007. Age, provenance, and regional correlation of the Athabasca Group, Saskatchewan and Alberta, constrained by igneous and detrital zircon geochronology; *In* C.W. Jefferson, and G. Delaney (eds), *EXTECH IV: Geology*

and Uranium EXploration TECHnology of the Proterozoic Athabasca Basin, Saskatchewan and Alberta; Geological Survey of Canada Bulletin 588, p. 193-209.

- Sader, J.A., Hattori, K.H., Kong, J.M., Hamilton, S.M., Brauneder, K., 2011. Geochemical responses in peat groundwater over Attawapiskat kimberlites, James Bay Lowlands, Canada, and their application to diamond exploration; *Geochemistry: Exploration, Environment and Analysis*. Vol. 11, p. 193-210.
- Schreiner, B.T., 1984a. Quaternary geology of the Precambrian Shield, Saskatchewan; Saskatchewan Energy and Mines Report 221, 106 p., 1 map, scale 1:1 000 000.
- Schreiner, B.T., 1984e. Quaternary geology of the Cree Lake area (NTS 74G), Saskatchewan; Saskatchewan Energy and Mines, Open File Report 84-12, scale 1:250 000.
- Smee, B.W. 1998. A new theory to explain the formation of soil geochemical responses over deeply covered gold mineralization in arid environments; *Journal of Geochemical Exploration*, Vol.61, p.149–172.
- de Smith, M.J., Goodchild, M.F., and Longley, P.A. 2008. *Geospatial Analysis – a comprehensive guide*, 2nd edition, The Winchelsea Press, <http://www.spatialanalysisonline.com/output>.
- Yeo, G. M., and Delaney, G., 2007. The Wollaston Supergroup, stratigraphy and metallogeny of a paleoproterozoic Wilson cycle in the Trans-Hudson Orogen, Saskatchewan; *In* C.W. Jefferson, and G. Delaney (eds), *EXTECH IV: Geology and Uranium EXploration TECHnology of the Proterozoic Athabasca Basin, Saskatchewan and Alberta*; Geological Survey of Canada Bulletin 588, p. 89-117
- Yeo, G.M., Jefferson, C.W., and Ramaekers, P., 2007. Comparison of lower Athabasca Group stratigraphy among depositional systems, Saskatchewan and Alberta; *In* *EXTECH IV: Geology and Uranium EXploration TECHnology of the Proterozoic Athabasca Basin, Saskatchewan and Alberta*, (ed.) C.W. Jefferson and G. Delaney; Geological Survey of Canada, Bulletin 588, p. 465-488.

Table 1: Sample location, pH and Conductivity of B- and E-horizon soil samples

Station	pH	Conductivity ($\mu\text{S}/\text{cm}$)	Easting	Northing
PHX001E	4.2	290	477236	6374448
PHX001B	4.3	444	477236	6374448
PHX002E	4.4	277	477251	6374441
PHX002B	4.8	290	477251	6374441
PHX003E	4.4	83	477259	6374432
PHX003B	4.7	408	477259	6374432
PHX004E	4.5	105	477269	6374425
PHX004B	4.9	45	477269	6374425
PHX005E	4.2	98	477273	6374414
PHX005B	5	40	477273	6374414
PHX006E	4.5	125	477288	6374397
PHX006B	5.4	28	477288	6374397
PHX007E	4.1	110	477290	6374396
PHX007B	5.1	55	477290	6374396
PHX008E	4.6	42	477301	6374383
PHX008B	4.6	97	477301	6374383
PHX009E	5.3	4	477316	6374389
PHX009B	5.3	15	477316	6374389
PHX010E	4.3	16	477321	6374379
PHX010B	5.3	4	477321	6374379
PHX011E	4.1	12	477329	6374379
PHX011B	4.8	16	477329	6374379
PHX012E	4.3	3	477333	6374370
PHX012B	4.9	6	477333	6374370
PHX013E	4.8	1	477343	6374365
PHX013B	4.7	2	477343	6374365
PHX014E	4.8	17	477350	6374367
PHX014B	5.2	8	477350	6374367
PHX015E	5.1	11	477362	6374364
PHX015B	5.4	10	477362	6374364
PHX016E	4.5	6	477374	6374368
PHX016B	5.3	6	477374	6374368
PHX017E	4.6	24	477387	6374381
PHX017B	4.6	33	477387	6374381
PHX018E	4.8	26	477396	6374381
PHX018B	5	29	477396	6374381
PHX019E	4.4	11	477405	6374387
PHX019B	5	15	477405	6374387
PHX020E	4.7	12	477416	6374392

Station	pH	Conductivity ($\mu\text{S}/\text{cm}$)	Easting	Northing
PHX020B	5	14	477416	6374392
PHX021E	5.2	5	477440	6374410
PHX021B	5	14	477440	6374410
PHX022E	5.2	4	477639	6374442
PHX022B	5.6	6	477639	6374442
PHX023E	5.3	32	476953	6373915
PHX023B	6.5	57	476953	6373915
PHX024E	5.5	11	476945	6373924
PHX024B	6	6	476945	6373924
PHX025E	5.3	12	476940	6373938
PHX025B	5.8	14	476940	6373938
PHX026E	5.9	18	476930	6373951
PHX026B	5	16	476930	6373951
PHX027E	4.6	10	476921	6373967
PHX027B	5.6	8	476921	6373967
PHX028E	4	8	476913	6373966
PHX028B	4.7	10	476913	6373966
PHX029E	4.1	3	476908	6373985
PHX029B	4.5	8	476908	6373985
PHX030E	3.8	10	476902	6373997
PHX030B	4.8	7	476902	6373997
PHX031E	3.8	7	476890	6374009
PHX031B	4.5	7	476890	6374009
PHX032E	4.1	4	476880	6374026
PHX032B	4.5	5	476880	6374026
PHX033E	4.2	14	476869	6374037
PHX033B	4.5	5	476869	6374037
PHX034E	4	2	476856	6374048
PHX034B	4.1	4	476856	6374048
PHX035E	3.7	5	476847	6374059
PHX035B	4.3	6	476847	6374059
PHX036E	3.6	4	476841	6374070
PHX036B	4.2	4	476841	6374070
PHX037E	4	2	476832	6374084
PHX037B	4.2	4	476832	6374084
PHX038E	3.9	5	476826	6374096
PHX038B	4.1	4	476826	6374096
PHX039E	4	5	476820	6374115
PHX039B	3.8	2	476820	6374115
PHX040E	3.7	7	476811	6374135
PHX040B	4.3	17	476811	6374135

Station	pH	Conductivity ($\mu\text{S}/\text{cm}$)	Easting	Northing
PHX041E	3.8	7	476853	6374110
PHX041B	4.3	1	476853	6374110
PHX042E	3.7	4	476863	6374103
PHX042B	4.1	8	476863	6374103
PHX043E	3.8	2	476872	6374090
PHX043B	3.8	10	476872	6374090
PHX044E	3.7	11	476882	6374084
PHX044B	4.1	7	476882	6374084
PHX045E	4	4	476889	6374065
PHX045B	3.9	10	476889	6374065
PHX046E	3.8	4	476901	6374066
PHX046B	4.3	2	476901	6374066
PHX047B	4.4	5	476908	6374048
PHX048B	3.6	2	476919	6374036
PHX049B	3.7	2	476931	6374026
PHX050B	3.6	4	476941	6374018
PHX051B	3.3	3	476950	6374008
PHX052B	3.3	2	476957	6374002
PHX053B	3.2	3	476963	6373995
PHX054B	3.3	7	476980	6373983
PHX055B	3.4	5	476992	6373966
PHX056B	N/A	12	477009	6373957
PHX057B	N/A	7	477017	6373939
PHX058B	N/A	4	477028	6373928
PHX059B	N/A	1	477053	6373904

Table 2: Detection Limits (DL) of the analytical methods

Method 1F-MS: Geochemical Ultratrace Aqua Regia Digestion (Acme Labs)

Analyte	Mo	Cu	Pb	Zn	Ag	Ni	Co	U	W
Unit	PPM	PPM	PPM	PPM	PPB	PPM	PPM	PPM	PPM
DL	0.01	0.01	0.01	0.1	2	0.1	0.1	0.1	0.1

Method 1SLE: Ammonium acetate sequential leach (Acme Labs)

Analyte	Mo	Cu	Pb	Zn	Ag	Ni	Co	U	W
Unit	PPB	PPB	PPB	PPB	PPB	PPB	PPB	PPB	PPB
DL	10	20	20	100	3	50	20	5	10

Method 1SLM: Hydroxylamine sequential leach (Acme Labs)

Analyte	Mo	Cu	Pb	Zn	Ag	Ni	Co	U	W
Unit	PPB	PPB	PPB	PPB	PPB	PPB	PPB	PPB	PPB
DL	10	20	20	100	3	50	20	5	10

Method ICPMS1: Sandstone Exploration Package (SRC Labs)

Analyte	Mo	Cu	Pb	Zn	Ag	Ni	Co	U	W
Unit	PPM	PPM	PPM	PPM	PPM	PPM	PPB	PPB	PPB
DL	0.02	0.1	0.02	1	0.02	0.1	0.02	0.02	0.1